Antiferromagnetism mediated by heavy electrons: High-order RKKY

Mi Jiang,[1] Jeroen Custers,[2] and Wenxin Ding[3]
[1]*Institute of Theoretical and Applied Physics, Jiangsu Key Laboratory of Thin Films, School of Physical Science and Technology, Soochow University, Suzhou 215006, China*
[2]*Faculty of Mathematics and Physics, Charles University in Prague, Ke Karlovu 5, 121 16 Prague 2, Czech Republic*
[3]*School of Physics and Optoelectric Engineering, Anhui University, Hefei, Anhui Province 230601, China*

(Received 29 May 2020; revised 31 January 2022; accepted 25 February 2022; published 23 March 2022)

Can the antiferromagnetic (AF) order be induced via the local moments' hybridization with the heavy electrons instead of conduction electrons? We address this intriguingly fundamental question via a prototypical model to describe the interplay between local moments and heavy electrons. We discover that the AF order can be mediated via the heavy electrons through the mechanism of the high-order Ruderman-Kittel-Kasuya-Yosida (RKKY) interaction. Moreover, our analysis employing a slave-spin representation uncovers that the heavy electron band can enhance the RKKY interaction of local moments (despiteits high-order nature) via enlarging its effective mass. The potential relevance to the heavy fermion compound $Ce_3(Pt/Pd)In_{11}$ is also discussed.

DOI: 10.1103/PhysRevResearch.4.013222

I. INTRODUCTION

The conventional Kondo/Anderson lattice model (KLM/PAM) describes the competition of antiferromagnetism and Kondo screening as a fundamental model of heavy fermion physics [1–6]. Generally, there are two well-known exchange mechanism responsible for the formation of the antiferromagnetic phase, i.e., (1) the superexchange interaction between localized electrons via their hybridization with the conduction band and (2) the Ruderman-Kittel-Kasuya-Yosida (RKKY) interaction originating from the scattering of the conduction electrons from two localized moments [7]. The former always favors the antiferromagnetic order between localized moment while the latter's sign and magnitude vary with the distance between localized moments and also the conduction band filling [8].

In KLM, the superexchange interaction is explicitly included as a Heisenberg interaction term among f moments while RKKY interaction is dynamically generated. In PAM, both terms are dynamically generated as effective interactions, hence their amplitudes would evolve as the system is tuned [9]. Nevertheless, for the conventional PAM, it is established that at small hybridization between the conduction and localized electrons, the indirect RKKY interaction induces the antiferromagnetic ground state, which competes with the paramagnetic spin liquid ground state formed by Kondo screening the local electrons by the conduction band at large hybridization.

The common thread between the aforementioned two exchange mechanism relies on the conduction electrons. It is natural to ask whether or not the heavy electrons can similarly act as a "glue" for the antiferromagnetic (AF) order between local moments. Until now, surprisingly, there has been few studies on this fundamental question despite that multiple $4f$ orbitals were accounted for in the context of cerium volume collapse considering the inherent $4f$ electronic correlations [10]. We point out that the AF order mediated by heavy electrons is not only an abstract theoretical question but also relevant to recent discovery of the microscopic coexistence between AF and superconductivity in a particular family of heavy fermion compounds $Ce_3(Pt/Pd)In_{11}$ harboring two inequivalent Ce sites [11–14], where the most fascinating scenario proposed for their coexistence claims that the Ce(1) sublattice is fully Kondo screened and responsible to the superconducting state while the Ce(2) sublattice forms the magnetic ordering. Therefore one intrinsic problem is the interplay between Ce(1) and Ce(2) sublattices, particularly the possible Ce(2) magnetic order induced by Ce(1) sublattice. Similar may as well apply to other systems with two crystallographic inequivalent f-electron sites, for instance, $Ce_3Pd_{20}Si_6$ [15], or artificially created f-electron superlattices [16–18].

Motivated by these experimental progress, in this proof of principle study, we explore the possibility of AF order mediated by heavy electrons via a prototypical model to describe the interplay between the local moments and heavy electrons. Specifically, we discover that the hybridization between the local moments and heavy electrons can indeed induce AF order between the local moments through the so-called high-order RKKY interaction that resembles the conventional one mediated via the conduction electrons in standard PAM/KLM.

II. MODEL AND METHODOLOGY

To illustrate our findings, we adopt the simplest and prototypical model consisting of two distinct localized f orbitals together with the conduction electrons on two-dimensional

square lattice, which reads in the half-filled form:

$$\mathcal{H} = -t\sum_{\langle ij\rangle\sigma}(c^\dagger_{i\sigma}c_{j\sigma} + c^\dagger_{j\sigma}c_{i\sigma}) - \mu\sum_{i\sigma}(n^c_{i\sigma} + n^{f_1}_{i\sigma} + n^{f_2}_{i\sigma}) + V\sum_{i\sigma}(c^\dagger_{i\sigma}f_{1i\sigma} + f^\dagger_{1i\sigma}c_{i\sigma}) + t_\perp\sum_{i\sigma}(f^\dagger_{1i\sigma}f_{2i\sigma} + f^\dagger_{2i\sigma}f_{1i\sigma}) + U\sum_{mi}\left(n^{f_m}_{i\uparrow} - \frac{1}{2}\right)\left(n^{f_m}_{i\downarrow} - \frac{1}{2}\right), \quad (1)$$

where $c^\dagger_{i\sigma}(c_{i\sigma})$ and $f^\dagger_{mi\sigma}(f_{mi\sigma})$ with $m = 1, 2$ are creation(destruction) operators for conduction and two local $f_{1,2}$ electrons on site i with spin σ. $n^{c,f_m}_{i\sigma}$ are the associated number operators. The chemical potential μ can be tuned for a desired average occupancy of three orbitals. The hopping $t = 1$ between conduction electrons on nearest neighbor sites $\langle ij\rangle$ sets the energy scale. U is the local repulsive interaction in the $f_{1,2}$ orbital. Note that in this work we only consider the case that the $f_{1,2}$ orbitals share an identical U for simplicity although generally they can differ. The two remaining control parameters are two distinct hybridizations, namely, V between c-f_1 and $t_\perp$ between f_1-f_2.

Before proceeding, we remark that in the heavy fermion compounds with multiple crystallographic inequivalent local moment sites, such as $Ce_3(Pt/Pd)In_{11}$ [11–14], the local environment of two Ce ions are different leading to distinct Kondo interaction strengths with the conduction electrons. Here our focus is on the sole effects of the heavy electrons from c-f_1 Kondo singlets on the additional f_2 local moments. Thus we neglect the c-f_2 hybridization to avoid the additional Kondo screening from c electrons and associated complexity. This crude simplification finds some justification. In the case of Ce_3PtIn_{11}, recent ^{115}In NQR experiments revealed that the ratio of magnetic moment between the Ce(1) site and Ce(2) is about 1/40, with Ce(2) yielding 1.72 μ_B [19] while neutron experiments on $Ce_3Pd_{20}Si_6$ showed that the magnetic ordering relates to the cubic Ce-8c site only, while the Ce-4a site remains "magnetically silent" [20]. Nevertheless, a more realistic modeling of the heavy fermion compounds is left for future investigation. In addition, to explicitly investigate the AF order without charge fluctuation, we stick on the half-filled systems by setting $\mu = 0$ so that the c and $f_{1,2}$ orbitals are individually half-filled.

To gather some initial insights of this model, it is worthwhile elaborating on some limiting cases. In the absence of Hubbard interaction U, the three-orbital unit cell gives rise to three energy bands such that the system hosts a metallic ground state for any finite $V, t_\perp$ at half-filling. As discussed later, turning on U opens the orbital-selective spectral gap. In the extreme case of $t_\perp \ll V$, the system separates into conventional PAM plus additional individual local moments; in contrary, if $t_\perp \gg V$, the system becomes a conduction band plus individual strongly bound dimers.

To fully take into account all the energy scales on the equal footing, we use the well established numerical technique of finite temperature determinant quantum Monte Carlo (DQMC) [21] to explore the physics of Eq. (1). As a celebrated computational method, DQMC provides an approximation-free solution in the presence of strong correlations. Besides, finite size scaling can facilitate the extraction of the AF order parameter reliably so that all the quantities throughout the paper are extracted values in the thermodynamic limit.

Throughout the paper, we concentrate on the characteristic intermediate coupling strength $U = 4.0t$, where it has been widely believed that the critical c-f hybridization strength separating the Kondo singlet and antiferromagnetic insulating ground states in PAM is $V_c \sim 1.0t$ [6,22]. Because the major purpose of this work is the AF order induced by heavy electrons, we only explore the systems with $V/t \geqslant 1.2$ such that the c-f_1 subsystem is readily within the heavy electron regime. Besides, all the physical quantities are obtained through finite-size scaling in lattice sizes as large as $N = 10 \times 10$ with periodic boundary at lowest temperature $T = 0.025t$.

Our major findings are illustrated in the tentative phase diagram Fig. 1 and summarized as follows.

(1) Singlet shielding (SS): f_2 local moments are effectively standing alone and shielded from the heavy electrons (c-f_1 singlets).

(2) f_2-AF: f_2 has the induced AF order via high-order RKKY mediated by c-f_1 heavy electrons.

(3) f_{12}-D: f_2's AF order disappears due to the confinement of the strong f_1-f_2 dimer formation.

Some remarks follow in order. First of all, f_1 orbital does not exhibit the AF order unless at relatively small $V/t = 1.2$ and 1.6 due to the twofold hybridization with c and f_2. Besides, at sufficiently large $t_\perp$, the strongly coupled f_1-f_2 dimers kill f_2's AF order and partly liberates the conduction electrons. In Fig. 1, in addition, the red dashed line highlights the $t_\perp$ at which the f_2-AF structure factor reaches its maximum. Note that the f_2-AF order rapidly turns on upon its emergence and gradually disappears with increasing $t_\perp$. In what follows, we provide the concrete numerical and analytical evidence to support the phase diagram in detail.

III. NUMERICAL RESULT

We illustrate our findings of the induced f_2-AF order mediated via heavy electrons (c-f_1 singlets) by the AF structure factor [23] of the $f_{1,2}$ local moments

$$S^{f_m}_{\rm AF} = \frac{1}{N}\sum_{ij} e^{-i\mathbf{q}\cdot(\mathbf{R_i}-\mathbf{R_j})}\left\langle\left(n^{f_m}_{i\uparrow} - n^{f_m}_{i\downarrow}\right)\left(n^{f_m}_{j\uparrow} - n^{f_m}_{j\downarrow}\right)\right\rangle \quad (2)$$

with $m = 1, 2$ at $\mathbf{q} = (\pi, \pi)$, where $\mathbf{R_i}$ denotes the coordinates of site i and N is the lattice size.

Figure 2(a) shows the finite-size scaling of $S^{f_m}_{\rm AF}/N$ at fixed $V/t = 2.0$ with dashed/solid lines denoting $m = 1$ and 2, respectively. Clearly, at small $t_\perp$, the c-f_1 singlets shields the additional f_2 local moments and the two subsystems are effectively separated so that both show absence of AF order. With increasing $t_\perp$, the f_2-AF order emerges while f_1 local moments remain forming the Kondo singlets with the conduction electrons, which indicates that the f_2-AF order is not induced by the proximity effect from a "f_1-AF" order liberated by the $t_\perp$ hybridization. In the standard PAM ($t_\perp = 0$), the RKKY interaction scales as $\sim J^2/W$ with $J \sim V^2/U$ and W the conduction bandwidth. Here we claim that f_2-AF is realized through a mechanism of high-order RKKY interaction via an indirect c-f_2 hybridization, for which we provide more detailed analysis in the next section. As expected, further

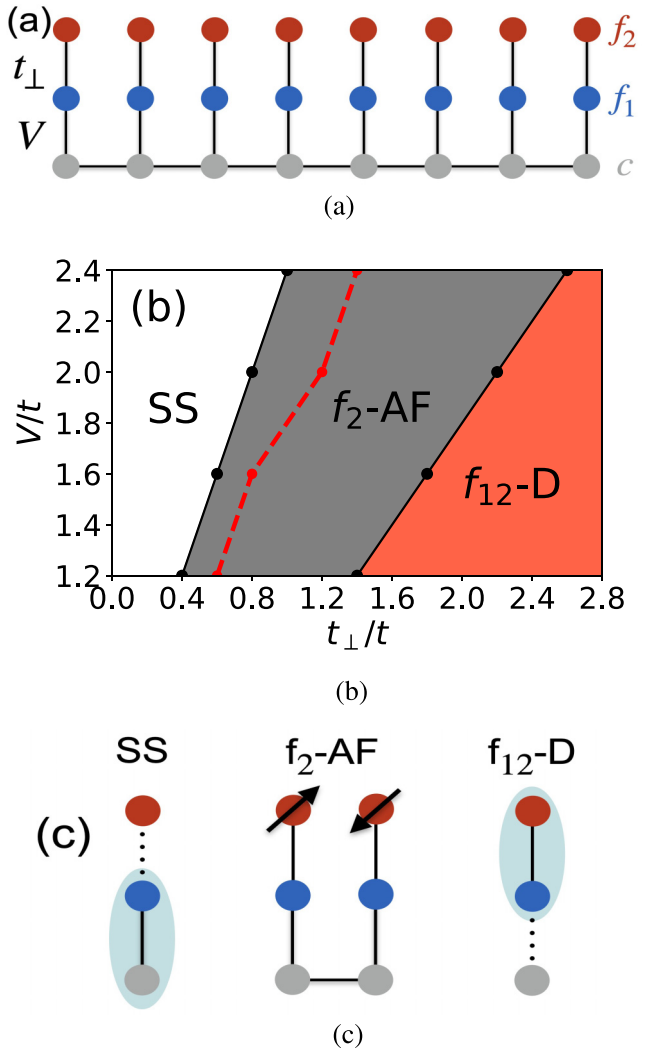

FIG. 1. (a) One-dimensional representation of the lattice geometry including c, f_1, and f_2 orbitals; (b) tentative phase diagram at half-filling for lowest simulated temperature $T = 0.025t$. The gray regimes exhibit the f_2-AF order mediated via heavy electrons formed via strong c-f_1 hybridization. The red dashed line highlights the specific $t_\perp$ locations with maximal AF structure factor (see text for details); (c) schematic representation of different phases, where the oval denotes the singlet formation and black arrows label the spin configuration forming the AF order for f_2 orbital.

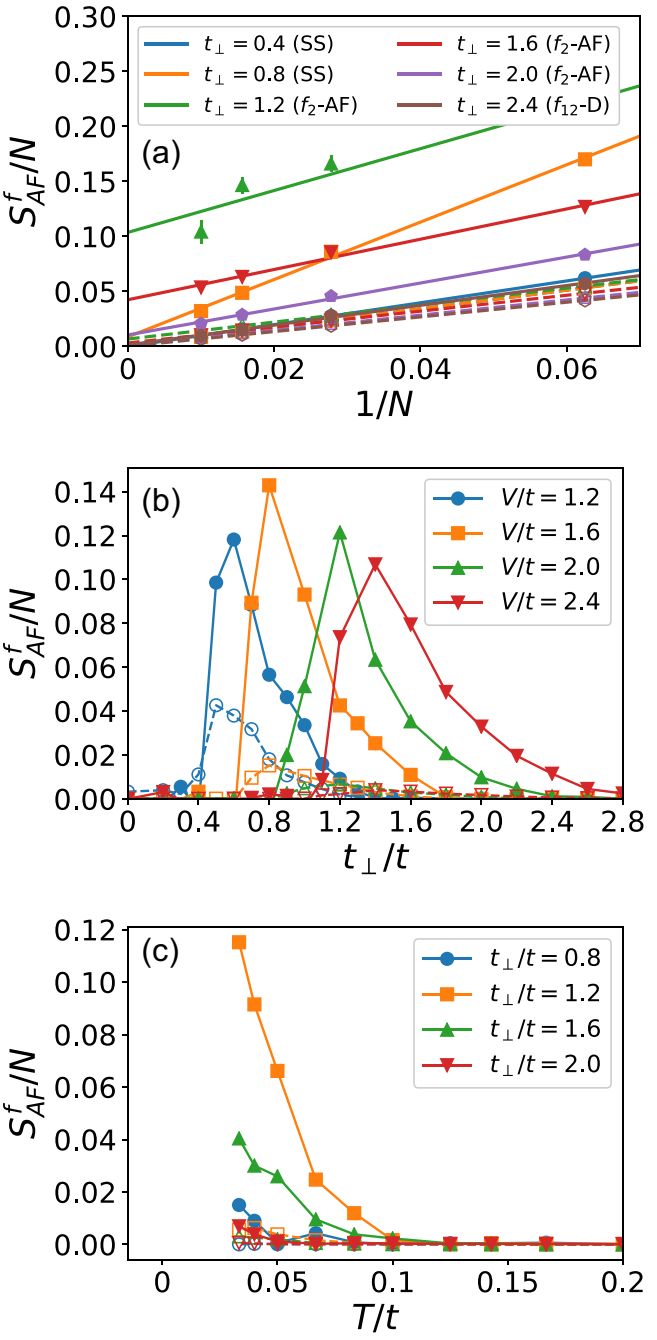

FIG. 2. (a) Finite-size scaling of $S^{f_m}_{\rm AF}/N$ at fixed $V/t = 2.0$. (b) Evolution of extrapolated $S^{f_m}_{\rm AF}/N$ with $t_\perp$ for diverse V at $T = 0.025t$. (c) Temperature dependence of extrapolated $S^{f_m}_{\rm AF}/N$ for various $t_\perp$ at fixed $V/t = 2.0$. The dashed (solid) lines are for f_1 (f_2) orbital.

increasing $t_\perp$ leads to the gradual diminish of f_2-AF due to the strong f_1-f_2 hybridization, which finally results in individual strongly bound dimers.

To make further progress, Fig. 2(b) demonstrates the evolution of the extrapolated $S^{f_m}_{\rm AF}/N$ with $t_\perp$ for diverse V, where the general peak structure of $S^{f_2}_{\rm AF}$ (solid lines) and the absence of f_1-AF order in most cases (dashed lines) can be seen. Additionally, the f_2-AF order rapidly turns on upon its emergence and gradually disappears, which reflects the robustness of the induced f_2-AF order and its struggling competition with f_1-f_2 hybridization $t_\perp$. It is natural that stronger V requires larger critical $t_\perp$ to overcome the c-f_1 Kondo screening to partially liberate the conduction electrons for its essential role in mediating the high-order RKKY that induces f_2-AF order. In contrary, only the systems of "light" heavy electrons with relatively small Kondo screening, e.g., $V/t = 1.2$, 1.6 (blue and orange dashed lines) clearly exhibit the f_1-AF order whose maximum are concomitant with that of f_2-AF. This observation indicates the feedback among c-f_1-f_2 orbitals: (a) $t_\perp$ tends to break the heavy electrons to liberate the c-electrons; (b) c electrons mediate the f_2-AF order via high-order RKKY; and (c) the induced f_2-AF order has proximity effect to induce the potential f_1-AF order unfavored by heavy electrons. Certainly,

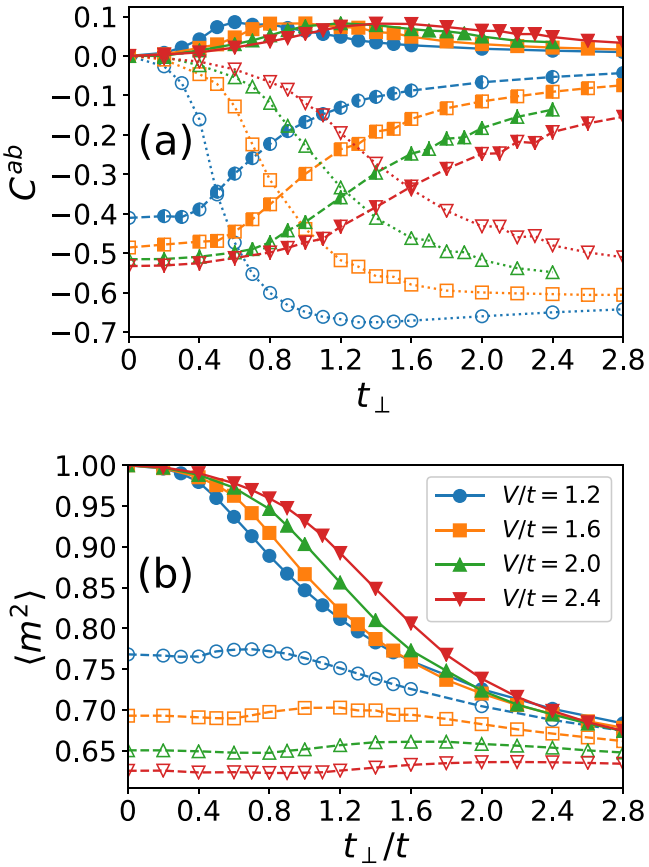

FIG. 3. (a) Local spin correlations C^{ab} between orbitals: C^{cf_2} (full symbols), C^{cf_1} (half-filled symbols), and $C^{f_1f_2}$ (unfilled symbols); (b) local moments $\langle m^2 \rangle$ of f_1 (dashed lines) and f_2 (solid lines) vs $t_\perp$ for diverse V at $T = 0.025t$.

the partially liberated c-electrons can also mediate the f_1-AF order to some extent, although their combined effects quickly decay with enlarging the c-f_1 hybridization V.

Figure 2(c) displays the temperature dependence of the extrapolated $S_{\rm AF}^{f_m}/N$ for various $t_\perp$ at fixed $V/t = 2.0$. Obviously, the f_2-AF order has different onset temperature scale, with $t_\perp/t = 1.2$ shows the highest starting temperature $T/t \sim 0.1$. The differing growth rate of $S_{\rm AF}^{f_2}$ with lowering T provides more evidence of the role of $t_\perp$ in inducing f_2-AF order.

To further support our scenario of high-order RKKY, we resort to the local static spin correlations

$$C^{ab} = \langle (n_\uparrow^a - n_\downarrow^a)(n_\uparrow^b - n_\downarrow^b) \rangle \tag{3}$$

between three orbitals $a, b = c, f_1, f_2$ in Fig. 3(a). Apparently, C^{cf_1} ($C^{f_1f_2}$) decreases (increases) in magnitude with turning on $t_\perp$. Nonetheless, the striking difference shows up in the indirect C^{cf_2} correlation, which exhibits a nontrivial peak, whose position is consistent with the maximal $S_{\rm AF}^{f_2}$ shown in Fig. 2. This strongly indicates that the "heavy" c electrons dressed by f_1 local moments are mediating the f_2-AF order in an indirect high-order manner. More careful comparison reveals that this common peak occurs at the specific $t_\perp$ where $C^{cf_1} \approx C^{f_1f_2}$ and also changes most rapidly. This observation implies that the homogeneous C^{cf_1} and $C^{f_1f_2}$ spin correlations are favored for enhancing C^{cf_2} and in turn strengthening the high-order RKKY interaction to mediate the f_2-AF order. In addition, the rapid evolution of C^{cf_1} and $C^{f_1f_2}$ in this regime reflects the crucial delicate balance between C^{cf_1} and $C^{f_1f_2}$. Furthermore, all these observations vividly implies the vital role of the heavy electrons (c-f_1 singlets) in mediating the f_2-AF order. Note that $|C^{cf_1}|$ gradually decreases and saturates at large enough $t_\perp$ while the f_2-AF order disappears, which implies that a "heavy" enough electrons (c-f_1 singlets) is requisite for mediating the f_2-AF order.

The essential physics of our model can be also described in the viewpoint of the competition and balance between $t_\perp$ and V, which can be explored by investigating another indicator of the magnetic properties, namely, the local moments $\langle m^2 \rangle = \langle (n_\uparrow^f - n_\downarrow^f)^2 \rangle$ of $f_{1,2}$. Figure 3(b) illustrates its behavior of f_1 (dashed lines) and f_2 (solid lines). Naturally, the f_2 local moment decreases with $t_\perp$, which is most rapidly in the regime where the f_2-AF order emerges. Nevertheless, the f_1 local moment does not vary much but only possesses a bump in the regime with the maximal f_2-AF order, which can be traced to its suppressed quantum fluctuation subject to twofold hybridization with c and f_2. This provides further evidence on the steadily frozen behavior of f_1 orbital, whose major role is to dress the c electrons.

IV. HIGH-ORDER RKKY

In the preceding section, we provided strong numerical evidence on the f_2-AF order induced by the c-f_1 heavy electrons. Moreover, we claimed that f_2-AF is realized through a mechanism of high-order RKKY interaction via an indirect c-f_2 hybridization.

Here we provide the derivation of this expectation analytically to leading order in V and $t_\perp$, which is realized by a dynamical t/U expansion [24] in a $U(1)$ slave-spin representation [25].

In this $U(1)$ slave-spin representation, the $f_{1(2)}$ fermions are written as a product of a spinon fermion $\tilde{f}_{1(2)}$ and a two-flavored slave-spin operator $\tau_{1,2}^{\pm}$ as

$$\begin{aligned} f_{mi\sigma} &= \tilde{f}_{mi\sigma}(\tau_{ma}^- + \tau_{mb}^-)/\sqrt{2}, \\ f_{mi\sigma}^\dagger &= \tilde{f}_{mi\sigma}(\tau_{\rm mia}^+ + \tau_{\rm mib}^+)/\sqrt{2}, \end{aligned} \tag{4}$$

where $m = 1$ and 2, $\tau_{\rm mis}^{\pm}$ are ladder operators of slave spins, and $\tilde{f}_{mi\sigma}$ is a fermionic spinon operator. The slave spin operators are regular $S = 1/2$ operators satisfying the SU(2) Lie algebra.

The U terms are mapped to an Ising interaction of the slave spins as $U n_{f_m,i\uparrow} n_{f_m,i\downarrow} \to U \tau_{\rm mia}^z \tau_{\rm mib}^z$. Therefore the slave spins describe the U-scale charge dynamics while the spinon fermions describe the magnetism. The V and $t_\perp$ terms are turned into vertexes between the spinons and slave spins. Then we integrate out the slave spins diagrammatically to obtain the effective spin-spin interactions, given in the form of four-spinon vertexes. A finite hybridization between $c - f_1$ is assumed for the calculation. The results are summarized in Table I. Details of the derivation are given in Appendix.

For the effective hopping factors, we ignore the geometry of the c or f_1 bands, focusing on their effective masses. Hence we make the following approximate replacements: $\langle c_i^\dagger c_j \rangle(\omega = 0) \propto m_c^*$, $\langle \tilde{f}_{1i}^\dagger \tilde{f}_{1j} \rangle(\omega = 0) \propto m_{f_1}^*$ according to the

TABLE I. Summary of effective spin-spin interactions among different orbitals. Only terms of interest are listed.

	s^c	S^{f_1}	S^{f_2}
s^c		$J_K^{cf_1} \propto V^2/U$	$J_K^{cf_2} \propto m_{f_1}^{*2} V^2/U$
S^{f_1}	...	$J_{f_1} \propto m_c^{*2} V^4/U$	$J_D^{f_1 f_2} \propto V^2/U$
S^{f_2}	...	...	$J_{f_2} \propto m_{f_1}^{*2} t_\perp^2 V^2/U$

mean-field solutions of Green's functions in a hybridized phase [26].

$$m_c^* \propto (m_{c,0}^{-1} + V^2/\lambda)^{-1} \simeq m_{c,0},$$
$$m_{f_1}^* \propto (\lambda + V^2/m_{c,0})^{-1}, \tag{5}$$

where $\lambda \sim T_K$ is a mean-field parameter. $\langle \tilde{f}_{1i}^\dagger \tilde{f}_{1j} \rangle$ is obtained in a mean-field sense, hence describes the heavy quasiparticle band formed by c-f_1 hybridization.

Through the above analysis, we find that the c-f_1 hybridization serves to enhance the high-order RKKY J_{f_2} and the Kondo interaction $J_K^{cf_2}$ with its large effective mass. This explains the mechanism of both f_2-fermions' suppression of the c-f_1 Kondo correlation and the development a stronger antiferromagnetism at intermediate $t_\perp$.

V. CONCLUSION

In conclusion, as a proof of principle study, we have addressed the fundamental question of whether or not the antiferromagnetic (AF) order can be induced via the local moments' hybridization with the heavy electrons instead of conduction electrons. We provided strong numerical evidence to confirm its possibility via a prototypical model through determinant QMC simulations. In particular, we claim that this AF order mediated by heavy electrons is realized by a so-called high-order RKKY interaction that resembles the conventional RKKY mediated via the conduction electrons in standard PAM/KLM. We emphasize that the induced AF order only emerges if the heavy electrons are present and moderately "heavy." Moreover, we provided the analytical confirmation on the high-order RKKY mechanism based on a dynamical t/U expansion in a U(1) slave-spin representation.

As our motivation partly came from the potential relevance to the heavy fermion compound $Ce_3(Pt/Pd)In_{11}$ [11–14], we remark that the three orbitals c, f_1, and f_2 in our prototypical model can be used to mimic Pt/Pd, Ce(1), and Ce(2) separately of $Ce_3(Pt/Pd)In_{11}$. Our findings implies that the experimentally observed magnetic ordering of Ce(2) (f_2 orbital) can indeed coexist microscopically with the fully Kondo screened Ce(1) (f_1 orbital) and in fact the Ce(1) plays a significant role in forming the AF order of Ce(2) sublattice. To some extent, however, our model has intrinsic limitation due to its neglecting of conduction electron reservoir from In sites because it has been shown that the strong hybridization with the out of plane In plays an important role in other Ce-based compounds, such as Ce-115 materials [27]. Therefore it is requisite to explore the more appropriate models for the potential connection of our findings reported here to the realistic materials, which is left for future investigation. Another fascinating theoretical question regards on the reverse role of Ce(2) on the superconductivity claimed experimentally to be responsible by Ce(1) [14]. Besides, the thorough understanding and realization of the proposed high-order RKKY interaction in other contexts would be highly interesting.

ACKNOWLEDGMENTS

M. Jiang acknowledge R. T. Scalettar for fruitful discussion and J. Custers acknowledges the discussion with G. Zwicknagl. M. Jiang was supported by National Natural Science Foundation of China (NSFC) Grant No. 12174278, the startup fund from Soochow University, and Priority Academic Program Development (PAPD) of Jiangsu Higher Education Institutions. M. Jiang also acknowledges Stewart Blusson Quantum Matter Institute of University of British Columbia in the initial stage of this work. J. Custers was supported by the Grant Agency of the Grant Agency of the Czech Republic (Project No. 18–23606S). W. Ding was supported by the Anhui Provincial Natural Science Foundation Young Scientist Grant No. 1908085QA35 and the Startup Grant No. S020118002/002 of Anhui University.

APPENDIX A: MORE DETAILS ON THE ANALYTICAL DERIVATION ON HIGH-ORDER RKKY

To compute spin-spin interactions in this model, we employ the U(1) slave-spin representation [25] of the Hubbard models to treat the U term and analyze the effective interactions between c, f_1 and f_2 spins perturbatively using a dynamical t/U expansion developed in Ref. [24].

In the slave spin representation, we rewrite the f fermions as a product of a spinon fermion and a two-flavored slave-spin operators as

$$f_{mi\sigma} = \tilde{f}_{mi\sigma}(\tau_{ma}^- + \tau_{mb}^-)/\sqrt{2},$$
$$f_{mi\sigma}^\dagger = \tilde{f}_{mi\sigma}(\tau_{\text{mia}}^+ + \tau_{\text{mib}}^+)/\sqrt{2}, \tag{A1}$$

where $m = 1, 2$, $\tau_{\text{mis}}^\pm$ are ladder operators of slave spins, and $\tilde{f}_{mi\sigma}$ is a fermionic spinon operator. The slave spin operators are regular $S = 1/2$ operators satisfying the SU(2) Lie algebra: $[\tau_{\text{mis}}^\alpha, \tau_{m'i's'}^\beta] = \delta_{mm'}\delta_{ii'}\delta_{ss'}\epsilon^{\alpha\beta\gamma}\tau_{\text{mis}}^\gamma$ with α, β, and γ run through x, y, and z, and the ladder operators are defined as $\tau_{\text{mis}}^\pm = \tau_{\text{mis}}^x \pm i\tau_{\text{mis}}^y$. Note that indices a and b are not associated with the physical spin index σ. The constraint between the spinons and the slave spins are

$$\sum_{s=a,b} \tau_{\text{mis}}^z = \sum_{\sigma=\uparrow,\downarrow} \left(\tilde{f}_{mi\sigma}^\dagger \tilde{f}_{mi\sigma} - \frac{1}{2} \right). \tag{A2}$$

The Hamiltonian of the f-band HM in this slave-spin representation is written as

$$H = H_{c,0} + H_{\tau,0} + H_{\tilde{f},0} + H_V + H_{t_\perp}, \tag{A3}$$

with

$$H_{c,0} = \sum_{ij\sigma} t_{ij} c_{i\sigma}^\dagger c_{j\sigma},$$
$$H_{\tau,0} = \frac{U}{2} \sum_{im} \Big(\sum_s \tau_{\text{mis}}^z \Big)^2 + h \sum_{\text{mis}} \tau_{\text{mis}}^z,$$

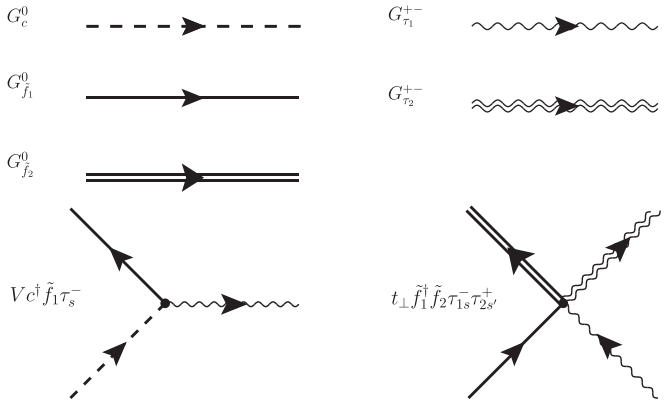

FIG. 4. Bare Green's functions and vertexes of the slave spin representation for $\mathcal{H}$ in Eq. (1).

$$H_V = V \sum_{i\sigma} c^\dagger_{i\sigma} \tilde{f}_{i\sigma} (\tau^-_{1ia} + \tau^-_{1ib}) + \text{H.c.}$$
$$H_{t_\perp} = -\sum_{\sigma} \frac{t_\perp}{2} (\tau^+_{1ia} + \tau^+_{1ib})(\tau^-_{2ia} + \tau^-_{2ib}) \tilde{f}^\dagger_{1i\sigma} \tilde{f}_{2i\sigma},$$
$$H_{\tilde{f},0} = (-h - \mu) \sum_{mi\sigma} n^{\tilde{f}}_{mi\sigma}. \tag{A4}$$

Here, μ is the chemical potential and h is a Lagrangian multiplier to implement the constraint.

At the zeroth order, consider the large- U limit, $H_{\tau,0}$ is solved in the atomic limit with $h = 0$:

$$iG[\tau^+_{mis}, \tau^-_{mjs'}](\nu; i, j) = \frac{\delta_{ij} \langle \tau^z_{mis} \rangle}{\nu - sU/2}. \tag{A5}$$

Details of correspondence between the slave spin at half-filling and the slave rotor representation are given in Ref. [25].

When H_V is turned on, we should obtain the conventional heavy fermi liquid as the ground state. In this slave spin representation, the mean-field solution of a heavy Fermi liquid is that $\langle \tau^x_{1is} \rangle \neq 0$ (or any direction in the xy plane). However, since we always keep $n_{f,i} = 1$, $h = 0$ will be preserved. In this case, the slave spins remain isotropic with respect to the flavor index s. From here on, we shall drop the s index and assume isotropy and summation over it to simplicity. With $\langle \tau^x_{1i} \rangle \neq 0$, the high-energy ($\sim U$) part of the slave spin dynamical correlation functions [Eq. (A5)] is also unchanged up to a renormalization factor $1 - \langle \tau^x_{1i} \rangle$.

The effective magnetic interactions can be obtained by contracting τs, treating H_V and $H_{t_\perp}$ as $\tilde{f}$-τ vertex. In a Lagrangian language, we can consider the procedure as "integrating out" the slave spins. We list the raw propagators and the vertexes as Feymann diagrams in Fig. 4.

For example, in the Hubbard model, the well-known superexchange interaction, which is the dimer interaction $J_{f_1 f_2}$ between f_1 and f_2 fermions mediated by $H_{t_\perp}$, is obtained by contracting the vertex at one-loop ($t^2_\perp$) level [24] as

$$H_{J^D} = \frac{J^D_{ij}}{2} f^\dagger_{i\alpha} f_{i\beta} f^\dagger_{j\beta} f_{j\alpha} \Rightarrow J_{ij} \boldsymbol{S}_i \cdot \boldsymbol{S}_j, \tag{A6}$$

where

$$J^D_{ij} = t^2_{ij} \int \frac{-d\omega}{2\pi} \sum_{ss'll'} G^{+-}_{S,ss'}[\omega, i, i] G^{-+}_{S,ll'}[\omega, j, j]. \tag{A7}$$

Plugging in the slave-spin Green's function at the atomic limit, we find the superexchange interaction at half-filling: $J_0 = 2t^2_{ij}/U$. The missing factor of 2 can be restored when taking into account the fluctuations of the hopping term similar as in Ref. [24].

The effective theory of Eq. (A3), assuming the $\langle \tau^x_1 \rangle \neq 0$, is analyzed as the following.

(1) First-order terms (V^2 and $t^2_\perp$):

(a) effective hopping of f_1 fermions:

$$H^{(1)}_{t,f_1} = \sum_{ij} V^2 t^{f_1}_{ij} \tilde{f}^\dagger_{1i} \tilde{f}_{1j} + \text{H.c.}, \tag{A8}$$

$$t^{f_1}_{ij} = \langle c^\dagger_j c_i \rangle (\omega = 0) = \int \frac{d^2\boldsymbol{k}}{4\pi^2} iG^0_c[\omega = 0; \boldsymbol{k}] e^{i\boldsymbol{k}\cdot\delta_{ij}}; \tag{A9}$$

(b) the Kondo term:

$$H^{(1)}_{K,c-f_1} = J^{cf_1}_K \boldsymbol{s}^c_i \cdot \boldsymbol{S}^{f_1}_i = \frac{J^{cf_1}_K}{2} \sum_{\alpha\beta} c^\dagger_{i\alpha} c_{i\beta} \tilde{f}^\dagger_{1i\beta} \tilde{f}_{1i\alpha}, \tag{A10}$$

with

$$J^{cf_1}_K = V^2 \sum_{ss'} iG[\tau^+_{mis}, \tau^-_{mis'}](\nu = 0; i, i) = V^2/U; \tag{A11}$$

(c) f_1-f_2 superexchange, H_{J^D} already given in Eq. (A6), $J^D_{ij} = 4t^2_\perp/U$. When $c - f_1$ hybridization is presentIn, a small correction factor $\sim 1 - \langle \tau^x_1 \rangle$ is expected.

(2) Second-order terms (V^4 or $t^4_\perp$):

(a) RKKY interaction between spins of f_1 fermions:

$$H^{(2)}_{J,f_1} = \sum_{ij} J_{f_1} \boldsymbol{S}^{f_1}_i \cdot \boldsymbol{S}^{f_1}_j, \tag{A12}$$
$$J_{f_1} = 4|t^{f_1}_{ij}|^2 V^4/U; \tag{A13}$$

(b) when c-f_1 hybridization is present, an effective three-leg vertex $\langle \tau^x_1 \rangle t_\perp \tilde{f}^\dagger_1 \tilde{f}_2 \tau^+_2$ emerges; it first induces an effective hopping for f_2 fermions:

$$H^{(2)}_{t,f_2} = \langle \tau^x_1 \rangle^2 t^2_\perp \sum_{ij} t^{f2}_{ij} \tilde{f}^\dagger_{2i\sigma} \tilde{f}_{2j\sigma} + \text{H.c.} \tag{A14}$$

with

$$t^{f_2}_{ij} = \langle \tilde{f}^\dagger_{1j} \tilde{f}_{1i} \rangle [\omega = 0] = \int d^2\boldsymbol{k}\, iG_{f_1}[\omega = 0; \boldsymbol{k}] e^{i\boldsymbol{k}\cdot\delta_{ij}}; \tag{A15}$$

consequently, $H^{(2)}_{t,f_2}$ opens two more channels of spin-spin interactions:

(i) higher order RKKY between f_2-fermion spins can be obtained akin Eq. (A12):

$$H^{(2)}_{J,f_2} = \sum_{ij} J_{f_2} \boldsymbol{S}^{f_2}_i \cdot \boldsymbol{S}^{f_2}_j, \tag{A16}$$
$$J_{f_2} = 4|t^{f_2}_{ij}|^2 t^4_\perp \langle \tau^x_1 \rangle^4 / U; \tag{A17}$$

(ii) also a higher order Kondo interaction between c and f_2 fermions:

$$H^{(2)}_{K,c-f_2} = J_K^{cf_2} \boldsymbol{s}_i^c \cdot \boldsymbol{S}_i^{f_2}, \tag{A18}$$

$$J_K^{cf_2} = \langle \tau_{1i}^x \rangle^2 V^2 |\langle \tilde{f}_{1i}^\dagger \tilde{f}_{1i} \rangle|^2 \times \sum_{ss'} iG[\tau_{mis}^+, \tau_{mis'}^-](\nu = 0) \propto t_\perp^2 V^2 \langle \tau_{1i}^x \rangle^2 / U. \tag{A19}$$

APPENDIX B: SPECTRAL PROPERTIES

In the main text, we focused on the magnetic properties, especially the f_2-AF order induced by c-f_1 heavy electrons. To further understand the phase diagram, we examined the spectral properties via the single-particle orbital-dependent local density of states (DOS) $N^a(\omega)$ with $a = c,\ f_1$, and f_2 relating to the local imaginary-time ordered Green's function $G^a(\tau) = \sum_{\mathbf{j}} \langle \mathcal{T} a_{\mathbf{j}}(\tau) a^\dagger_{\mathbf{j}\pm}(0) \rangle$ via

$$G^a(\tau) = \int_{-\infty}^{\infty} d\omega \frac{e^{-\omega\tau}}{e^{-\beta\omega}+1} N^a(\omega). \tag{B1}$$

To avoid the ambiguity from analytical continuation such as maximum entropy method [28], we resort to the approximate formula $N^a(\omega = 0) \approx \beta G^a(\tau = \beta/2)/\pi$ assuming that the temperature is much lower than the energy scale on which there are structures in DOS [29].

As shown in Fig. 5(a), the dominant feature exhibits at large $t_\perp \geqslant V$, where both c and f_2 orbitals display the metallic behavior while f_1 orbital is readily insulating in all regimes of the phase diagram. The strong metallicity of the conduction electron can be easily understood as the consequence of significantly weakened c-f_1 spin correlation (Fig. 3) that liberates the c electrons so that $\beta G^c(\beta/2)$ grows with $t_\perp$ until its ultimate saturation. Figure 5(b) provides more evidence by illustrating the imaginary-time dependence of $G(\tau)$ of three orbitals $c,\ f_1$, and f_2 in a specific case of large enough $t_\perp$, which clearly indicates the steadily insulating behavior of f_1.

Apparently, the most "unexpected" feature is the different spectral behavior between f_1 and f_2, which should naively behave similarly at large $t_\perp$. Strikingly, the comparison with Fig. 2 demonstrates that the metallicity of f_2 starts within the phase with f_2-AF order in Fig. 1. For instance, for $V/t = 1.6$, the f_2-AF regime occurs within $t_\perp/t \in [0.6, 1.8]$; while its metallicity starts from $t_\perp/t \sim 1.2$. Therefore, at relatively large $t_\perp$, the gray f_2-AF phase consists of a crossover from f_2 's AF insulating to metallic AF nature.

On the one hand, at small enough $t_\perp$, the perfect nesting of c electron's Fermi surface in our half-filled system and the strong c-f_1 hybridization V results in the insulating c-f_1 singlets, which has minor impact on the individual insulating f_2. On the other hand, at large enough $t_\perp$, the strongly bound f_1-f_2 dimers results in their common insulating feature. Although not explicitly shown in Fig. 5(a), we confirm that $\beta G^{f_2}(\beta/2)$ finally vanishes at sufficiently large $t_\perp$, whose trend can be clearly seen as its decrease with enlarging $t_\perp$.

In the intermediate $t_\perp$, we believe that the key difference between f_2's metallicity and f_1's insulating originates from

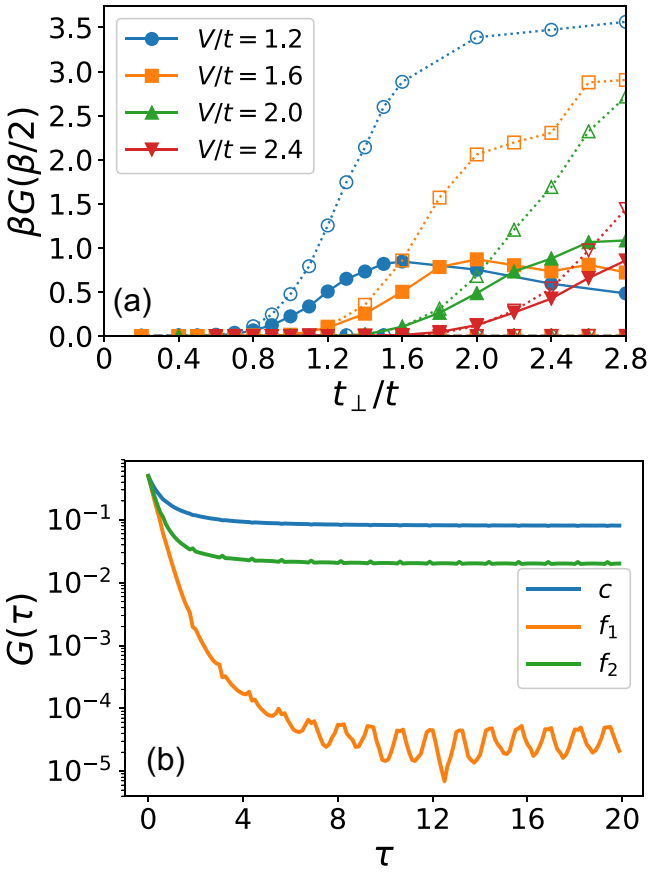

FIG. 5. (a) Approximate local DOS at Fermi level of three orbitals f_2 (full symbols), f_1 (half-filled symbols), and c (unfilled symbols) vs $t_\perp$ for diverse V at $T = 0.025t$. (b) The imaginary-time dependence of $\ln G^a(\tau)$ at $\tau \in [0, \beta t/2]$ for three orbitals $c,\ f_1$, and f_2 for $V/t = 1.6,\ t_\perp/t = 2.8$ [deep in the f_{12}-D regime of the phase diagram Fig. 1(b)] and $\beta t = 40.0$.

their different local hybridization. As shown in Fig. 2(b), the presence of f_2-AF accompanies with the much weaker f_1-AF. This AF correlation together with the perfect nesting of c electron's Fermi surface and the local f_1-f_2 hybridization gap out f_1 fermion at half-filling. In contrast, as derived in Appendix A, f_2's effective magnetic interaction is mediated by f_1, which does not have a nested Fermi surface since its effective hopping is proportional to $G_c[i, j] = \langle c_j^\dagger c_i \rangle$ so that f_2's metallicity is natural. Because the onset of f_2's metallicity starts from the weakened f_2-AF regime, this metallicity probably participates in destroying the f_2-AF order. Besides, the simultaneous onset of the metallicity of c and f_2 also indicates the importance of higher order c-f_2 hybridization induced by f_1.

Intuitively, the distinct difference between f_1 and f_2 reflects the more freedom of f_2 despite of the gradually stronger f_1-f_2 binding, which is consistent with the smooth(rapid) variation of $f_1(f_2)$ local moment with $t_\perp$ in Fig. 3(b). Despite of these suggestive discussion, we remark that how f_1 remains gapped throughout the phase diagram and also how f_2 shows metallicity at intermediate $t_\perp$ may need further investigation, particularly in the realistic settings of relevant materials, which is still unclear.

[1] P. W. Anderson, Localized magnetic states in metals, Phys. Rev. **124**, 41 (1961).

[2] S. Doniach, The Kondo lattice and weak antiferromagnetism, Physica B **91**, 231 (1977); B. Cornut and B. Coqblin, Influence of the crystalline field on the Kondo effect of alloys and compounds with cerium impurities, Phys. Rev. B **5**, 4541 (1972).

[3] G. R. Stewart, Heavy-fermion systems, Rev. Mod. Phys. **56**, 755 (1984).

[4] P. A. Lee, T. M. Rice, J. W. Serene, L. J. Sham, and J. W. Wilkins, Theories of heavy-electron systems, Comments Condens. Matter Phys. **12**, 99 (1986).

[5] A. Georges, G. Kotliar, W. Krauth, and M. J. Rozenberg, Dynamical mean-field theory of strongly correlated fermion systems and the limit of infinite dimensions, Rev. Mod. Phys. **68**, 13 (1996).

[6] T. Schafer, A. A. Katanin, M. Kitatani, A. Toschi, and K. Held, Quantum Criticality in the Two-Dimensional Periodic Anderson Model, Phys. Rev. Lett. **122**, 227201 (2019).

[7] A. N. Tahvildar-Zadeh, M. Jarrell, and J. K. Freericks, Protracted screening in the periodic Anderson model, Phys. Rev. B **55**, R3332(R) (1997).

[8] R. M. Fye, Quantum Monte Carlo study of the one-dimensional symmetric Anderson lattice, Phys. Rev. B **41**, 2490 (1990).

[9] O. Howczak and J. Spałek, J. Phys, Anderson lattice with explicit Kondo coupling revisited: metamagnetism and the field-induced suppression of the heavy fermion state, J. Phys.: Condens. Matter **24**, 205602 (2012).

[10] K. Held, A. K. McMahan, and R. T. Scalettar, Cerium Volume Collapse: Results from the Merger of Dynamical Mean-Field Theory and Local Density Approximation, Phys. Rev. Lett. **87**, 276404 (2001).

[11] J. Prokleska, M. Kratochvilova, K. Uhlirova, V. Sechovsky, and J. Custers, Magnetism, superconductivity, and quantum criticality in the multisite cerium heavy-fermion compound Ce_3PtIn_{11}, Phys. Rev. B **92**, 161114(R) (2015).

[12] M. Kratochvilova, J. Prokleska, K. Uhlirova, V. Tkac, M. Duse, V. Sechovsky, and J. Custers, Coexistence of Antiferromagnetism and Superconductivity in Heavy Fermion Cerium Compound Ce_3PdIn_{11}, Sci. Rep. **5**, 15904 (2015).

[13] D. Das, D. Gnida, L. Bochenek, A. Rudenko, M. Daszkiewicz, and D. Kaczorowski, Magnetic field driven complex phase diagram of antiferromagnetic heavy-fermion superconductor Ce_3PtIn_{11}, Sci. Rep. **8**, 16703 (2018).

[14] S. Kambe, H. Sakai, Y. Tokunaga, R. E. Walstedt, M. Kratochvílová, K. Uhlířová, and J. Custers, ^{115}In NQR study with evidence for two magnetic quantum critical points in dual Ce site superconductor Ce_3PtIn_{11}, Phys. Rev. B **101**, 081103(R) (2020).

[15] J. Custers, K-A. Lorenzer, M. Muller, A. Prokofiev, A. Sidorenko, H. Winkler, A. M. Strydom, Y. Shimura, T. Sakakibara, R. Yu, Q. Si, and S. Paschen, Destruction of the Kondo effect in the cubic heavy-fermion compound $Ce_3Pd_{20}Si_6$, Nat. Mater. **11**, 189 (2012).

[16] H. Shishido, T. Shibauchi, K. Yasu, T. Kato, H. Kontani, T. Terashima, and Y. Matsuda, Tuning the dimensionality of the heavy fermion compound $CeIn_3$, Science **327**, 980 (2010).

[17] Y. Mizukami, H. Shishido, T. Shibauchi, M. Shimozawa, S. Yasumoto, D. Watanabe, M. Yamashita, H. Ikeda, T. Terashima, H. Kontani *et al.*, Extremely strong coupling superconductivity in artificial two-dimensional Kondo lattices, Nat. Phys. **7**, 849 (2011).

[18] S. K. Goh, Y. Mizukami, H. Shishido, D. Watanabe, S. Yasumoto, M. Shimozawa, M. Yamashita, T. Terashima, Y. Yanase, T. Shibauchi *et al.*, Anomalous Upper Critical Field in $CeCoIn_5/YbCoIn_5$ Superlattices with a Rashba-Type Heavy Fermion Interface, Phys. Rev. Lett. **109**, 157006 (2012).

[19] N. Shioda, K. Kumeda, H. Fukazawa, T. Ohama, Y. Kohori, D. Das, J. Blawat, D. Kaczorowski, and K. Sugimoto, Determination of the magnetic **q** vectors in the heavy fermion superconductor Ce_3PtIn_{11}, Phys. Rev. B **104**, 245119 (2021).

[20] P. Y. Portnichenko, A. S. Cameron, M. A. Surmach, P. P. Deen, S. Paschen, A. Prokofiev, J.-M. Mignot, A. M. Strydom, M. T. F. Telling, A. Podlesnyak, and D. S. Inosov, Momentum-space structure of quasielastic spin fluctuations in $Ce_3Pd_{20}Si_6$, Phys. Rev. B **91**, 094412 (2015).

[21] R. Blankenbecler, D. J. Scalapino, and R. L. Sugar, Monte Carlo calculations of coupled boson-fermion systems. I, Phys. Rev. D **24**, 2278 (1981).

[22] W. Hu, R. T. Scalettar, E. W. Huang, and B. Moritz, Effect of an additional conduction band on singlet-antiferromagnet competition in the periodic Anderson model, Phys. Rev. B **95**, 235122 (2017).

[23] The AF structure factor $S^f_{\rm AF}$ is a static $\omega = 0$ property. The more involved dynamical spin susceptibility $\chi(\mathbf{q} = (\pi, \pi))$ shows the similar behavior with $S^f_{\rm AF}$. In DQMC method adopted here, the calculation of χ requires the evaluation of imaginary-time dependence of the spin-spin correlations, which is much more time-consuming than the sole calculation of the static quantities like $S^f_{\rm AF}$.

[24] W. Ding, R. Yu, Q. Si, and E. Abrahams, Effective exchange interactions for bad metals and implications for iron-based superconductors, Phys. Rev. B **100**, 235113 (2019).

[25] W. Ding and R. Yu, Dynamical t/U Expansion of the Doped Hubbard Model, arXiv:1906.12071.

[26] P. Coleman, *Heavy Electrons, in Introduction to Many-Body Physics* (Cambridge University Press, 2015), pp. 656–719.

[27] K. Haule, C. Yee, and K. Kim, Dynamical mean-field theory within the full-potential methods: Electronic structure of $CeIrIn_5$, $CeCoIn_5$, and $CeRhIn_5$, Phys. Rev. B **81**, 195107 (2010).

[28] J. E. Gubernatis, M. Jarrell, R. N. Silver, and D. S. Sivia, Quantum Monte Carlo simulations and maximum entropy: Dynamics from imaginary-time data, Phys. Rev. B **44**, 6011 (1991).

[29] N. Trivedi and M. Randeria, Deviations from Fermi-Liquid Behavior above Tc in 2D Short Coherence Length Superconductors, Phys. Rev. Lett. **75**, 312 (1995).